ISSN 1674-1056
http://cpb.iphy.ac.cn
http://iopscience.iop.org/cpb
中国物理 B
Chinese Physics
中国物理 Chinese Physics B

Sb_2Te_3 mode-locked ultrafast fiber laser at 1.93 μm

Jintao Wang(王金涛), Jinde Yin(尹金德), Tingchao He(贺廷超), Peiguang Yan(闫培光)
Citation: Chin. Phys. B . 2018, 27(8): 084214. **doi:** 10.1088/1674-1056/27/8/084214

Journal homepage: http://cpb.iphy.ac.cn; http://iopscience.iop.org/cpb

What follows is a list of articles you may be interested in

Reduced graphene oxide as saturable absorbers for erbium-doped passively mode-locked fiber laser

Zhen-Dong Chen(陈振东), Yong-Gang Wang(王勇刚), Lu Li(李 璐), Rui-Dong Lv(吕瑞东), Liang-Lei Wei(韦良雷), Si-Cong Liu(刘思聪), Jiang Wang(王 江), Xi Wang(王茜)
Chin. Phys. B . 2018, 27(8): 084206. **doi:** 10.1088/1674-1056/27/8/084206

Generation of single and multiple dissipative soliton in an erbium-doped fiber laser

Li-Na Duan(段利娜), Jin Wen(文进), Wei Fan(樊伟), Wei Wang(王炜)
Chin. Phys. B . 2017, 26(10): 104205. **doi:** 10.1088/1674-1056/26/10/104205

Fiber fuse behavior in kW-level continuous-wave double-clad field laser

Jun-Yi Sun(孙骏逸), Qi-Rong Xiao(肖起榕), Dan Li(李 丹), Xue-Jiao Wang(王雪娇), Hai-Tao Zhang(张海涛), Ma-Li Gong(巩马理), Ping Yan(闫平)
Chin. Phys. B . 2016, 25(1): 014204. **doi:** 10.1088/1674-1056/25/1/014204

Yb-doped passively mode-locked fiber laser with Bi_2Te_3-deposited

Li Lu, Yan Pei-Guang, Wang Yong-Gang, Duan Li-Na, Sun Hang, Si Jin-Hai
Chin. Phys. B . 2015, 24(12): 124204. **doi:** 10.1088/1674-1056/24/12/124204

Passive harmonic mode-locking of Er-doped fiber laser using CVD-grown few-layer MoS_2 as a saturable absorber

Xia Han-Ding, Li He-Ping, Lan Chang-Yong, Li Chun, Deng Guang-Lei, Li Jian-Feng, Liu Yong
Chin. Phys. B . 2015, 24(8): 084206. **doi:** 10.1088/1674-1056/24/8/084206

SPECIAL TOPIC — Nanophotonics

Sb_2Te_3 mode-locked ultrafast fiber laser at 1.93 μm *

Jintao Wang(王金涛)[1,2], Jinde Yin(尹金德)[1,2], Tingchao He(贺廷超)[3], and Peiguang Yan(闫培光)[1,†]

[1] Shenzhen Key Laboratory of Laser Engineering, Key Laboratory of Advanced Optical Precision Manufacturing Technology of Guangdong Higher Education Institutes, College of Optoelectronic Engineering, Shenzhen University, Shenzhen 518060, China

[2] Key Laboratory of Optoelectronic Devices and Systems of Ministry of Education and Guangdong Province, College of Optoelectronic Engineering, Shenzhen University, Shenzhen 518060, China

[3] College of Physics and Energy, Shenzhen University, Shenzhen 518060, China

(Received 11 April 2018; revised manuscript received 7 May 2018; published online 25 July 2018)

Ultrafast pulse generation was demonstrated in thulium doped fiber laser mode locked by magnetron sputtering deposited Sb_2Te_3 with the modulation depth, non-saturable loss, and saturable intensity of 38%, 31.2%, and 3.3 MW/cm^2, respectively. Stable soliton pulses emitting at 1930.07 nm were obtained with pulse duration of 1.24 ps, a 3-dB spectral bandwidth of 3.87 nm, an average output power of 130 mW, and signal-to-noise ratio (SNR) of 84 dB. To our knowledge, this is the first demonstration of Sb_2Te_3-based SA in fiber lasers at 2-μm regime.

Keywords: fiber lasers, mode locking, nonlinear optical material

PACS: 42.55.Wd, 42.60.Fc, 42.70.Nq **DOI:** 10.1088/1674-1056/27/8/084214

1. Introduction

Ultrafast pulses operating at 2-μm region have received enormous attention due to their important applications such as materials processing, micromachining, and medicine.[1,2] It has been demonstrated that the ultrafast pulses could be generated efficiently by inserting a saturable absorber (SA) in a passively mode-locked fiber laser. Up to now, Various SAs were utilized to generate ultrafast pulses at different wavelengths.[3–30] Among these SAs, topological insulators (TIs) are particularly interesting due to the extraordinary charge and spin properties on the edge or surface modes of TIs. Unlike extensively studied graphene, TIs have the characteristics with a small band gap in the bulk state and a gapless metallic state in the surface.[31,32] The combination of the small bandgap bulk (0.2 eV∼ 0.3 eV) and the gapless surface enables TIs to possess an ultra-broad bandwidth of saturable absorption operation,[15] which can cover the mid-infrared spectral region. Sb_2Te_3, a typical TIs, has been successfully served as a SA in ultrafast fiber lasers[31] due to its superior saturable absorption feature and giant third order nonlinear optical property. However, the studies for its nonlinear optical property were mainly focused on 1.5-μm regime. Therefore, we believe that it would be technically meaningful to perform another systematic investigation on the applicability of Sb_2Te_3-based SAs for the implementation of 2-μm pulsed fiber lasers.

Generally, two-dimensional (2D) materials could be prepared via mechanical exfoliation (ME), liquid phase exfoliation (LPE), chemical vapor deposition (CVD), or magnetron-sputtering deposition (MSD).[33] 2D material obtained with LPE or ME methods usually have an uncontrollable size and random thickness, which are detrimental for the performance of a SA. CVD method could prepare 2D material with a large area and certainly atomic thickness,[34] but the preparation process is relatively complex (e.g., the 2D material films require to be carefully transferred onto target substrates and difficult to remove transfer residues completely). Compared with ME, LPE and CVD method, the MSD is a simpler method to grow 2D material on target substrates directly and suitable for mass-production, which are critical for their practical applications. Therefore, magnetron sputtering deposited Sb_2Te_3 was selected as the SA in the work. In order to enhance the reliability of the Sb_2Te_3 SA, the Sb_2Te_3 material was deposited directly on the waist of the microfiber. The microfiber-based Sb_2Te_3 SA with evanescent wave interaction is attractive for high power tolerance, which is benefit to generate high output power. Moreover, the whole microfiber (up to centimeter order) was completely coated tightly with the Sb_2Te_3 film, which ensures the strong nonlinear optical response in material together with the longer interaction length.

In this paper, we developed a type of microfiber-based Sb_2Te_3 SA with the MSD method, and then incorporated it into thulium doped fiber laser to generate stable ultrafast

*Project supported by the National Natural Science Foundation of China (Grant Nos. 61775146, 11704260, 61405126, and 61605122), the Shenzhen Science and Technology Project (Grant Nos. JCYJ20160427105041864, JSGG20160429114438287, KQJSCX20160226194031, JCYJ20160422103744090, and JCY20150324141711695), and the Natural Science Foundation of Guangdong Province, China (Grant Nos. 2016A030310049, 2016A030310059, and 2017A030310402).

†Corresponding author. E-mail: yanpg@szu.edu.cn

© 2018 Chinese Physical Society and IOP Publishing Ltd

pluses at 2 μm. Stable soliton pulses emitting at 1930.07 nm were obtained with pulse duration of 1.24 ps, a 3-dB spectral bandwidth of 3.87 nm, an average output power of 130 mW, and signal-to-noise ratio (SNR) of 84 dB. To our knowledge, this is the first demonstration of Sb_2Te_3-based SA in fiber lasers at 2-μm regime.

2. Fabrication and characterization

The preparation process of microfiber-based Sb_2Te_3 SA was briefly explained as follows. Firstly, the microfibers with effective fused zone length of about 1 cm and waist diameter of about 20 μm were obtained by stretching single mode fibers (SMF-28e) on a taper drawing machine. Then Sb_2Te_3 film was deposited onto the waist of microfibers by MSD technique. Briefly, the microfibers and the Sb_2Te_3 target with purity of 99.99% were placed into the vacuum chamber. A mechanical pump is firstly used to ensure that the vacuum degree reached 1.0×10^{-1} Pa in the vacuum chamber. Then the vacuum degree was pulled to 9.8×10^{-4} pa by using a molecular pump. After that, ionized Ar is excited by a pulsed direct-current (DC) power to bombard the Sb_2Te_3 target. The inspired Sb_2Te_3 plasma plume is then deposited onto the microfibers gradually. During the depositing process, the microfibers are rotated with the speed of 20 r/min to ensure the uniformity of Sb_2Te_3 film. For checking the Raman shift property of the Sb_2Te_3 film grown by MSD method, the thickness-dependent Raman spectrum is measured with a Raman spectrometer (Horiba, Raman Evolution hr800) excited by a 488-nm laser. Figure 1(a) shows the typical Raman spectra of Sb_2Te_3 films in the range from 100 cm^{-1} to 500 cm^{-1}. The main peaks are located at about 118 cm^{-1}, 250 cm^{-1}, and 450 cm^{-1}, which are in good agreement with the Raman peaks observed in V–VI compound semiconductors.[35] The peak at 118 cm^{-1} has been identified as the E_g vibrational mode. The weak shoulders at 138 cm^{-1}, 159 cm^{-1}, 189 cm^{-1}, and 371 cm^{-1} are probably from the secondary phase such as (Sb, O) in the film. In addition, its nonlinear absorption coefficient β and the nonlinear refractive index n_2 are determined with the Z-scan technique. A mode-locked Ti:sapphire oscillator-seeded regenerative amplifier is used to generate femtosecond pulses with a central wavelength of 800 nm, pulse duration of 100 fs, and repetition rate of 1 kHz. The open aperture (OA) Z-scan measurement is shown in Fig. 1(b). Typical saturable absorption curve is observed, demonstrating the effective saturable absorption at 800 nm. As for OA Z-scan, the normalized transmittance can be expressed as[36]

$$T(z)=\sum_{m=0}^{\infty}\frac{\left[\dfrac{-\beta I_0 L_{\text{eff}}}{1+z^2/z_0^2}\right]^m}{(m+1)^{3/2}}, \tag{1}$$

where, I_0 is peak intensity at the focus, z is the position of the sample with respect to the focal position, z_0 is the diffraction length of the beam. The effective length of the sample L_{eff} could be obtained with the following equation

$$L_{\text{eff}}=\left(1-\mathrm{e}^{-\alpha_0 L}\right)/\alpha_0, \tag{2}$$

where L is the sample thickness, α_0 is the line absorption coefficient. As a result, the fitting parameter β could be unambiguously deduced by fitting the experimental data with Eq. (1). Besides, the closed aperture (CA) Z-scan measurement is also measured to estimate the nonlinear refractive index of Sb_2Te_3 film. The typical CA/OA curve is shown in Fig. 1(c). The Sb_2Te_3 film showed the feature of peak-valley profile, meaning that the sample is self-defocusing with a negative nonlinear refractive index. The experimental data can be fitted by using the following equation[37]

$$\begin{aligned}T(x) = 1&+\frac{4x\Delta\phi}{(1+x^2)(9+x^2)}+\frac{4\left(3x^2-5\right)\Delta\phi^2}{(1+x^2)^2(9+x^2)(25+x^2)}\\&+\frac{32\left(3x^2-11\right)x\Delta\phi^3}{(1+x^2)^3(9+x^2)(25+x^2)(49+x^2)},\end{aligned} \tag{3}$$

where $T(x)$ is the normalized transmittance, $x=z/z_0$. The only fitting parameter $\Delta\phi$ could be obtained through Eq. (3). Therefore, the refractive index n_2 can be deduced by using the following equation

$$n_2=\Delta\phi/kI_0L_{\text{eff}}, \tag{4}$$

where $k=2\pi/\lambda$ is the wave vector. In our experiments, the parameters of β and n_2 were estimated to be about 9.0×10^4 cm/W and -8.0×10^8 cm^2/W according to the actual experimental data points, respectively. The resulting value of β for Sb_2Te_3 is much higher than those of graphene oxide,[38] MXene,[39] transitionmetal dichalcogenide MoS_2,[40] and black phosphorus,[41] indicating a strong optical switch capability of Sb_2Te_3. The higher β value of Sb_2Te_3 also indicated that it could be exploited as potential material for nanophotonic devices, especially optical limiter.[42] Furthermore, the recovery time of Sb_2Te_3 material is measured by using a pump-probe experiment. Figure 1(d) presents carriers dynamic relaxation process with the pump and probe wavelength of 400 nm. Its dynamic relaxation process exhibits an exponential decay. The process is fitted by exponential decay function of $y=A*\exp(-(x-x_0)/\tau)+y_0$, where τ represents the fast relaxation time during dynamic relaxation. The fast relaxation time is calculated to be about 5 ps with the theoretically fitting, showing the ultrafast response of the Sb_2Te_3 material.

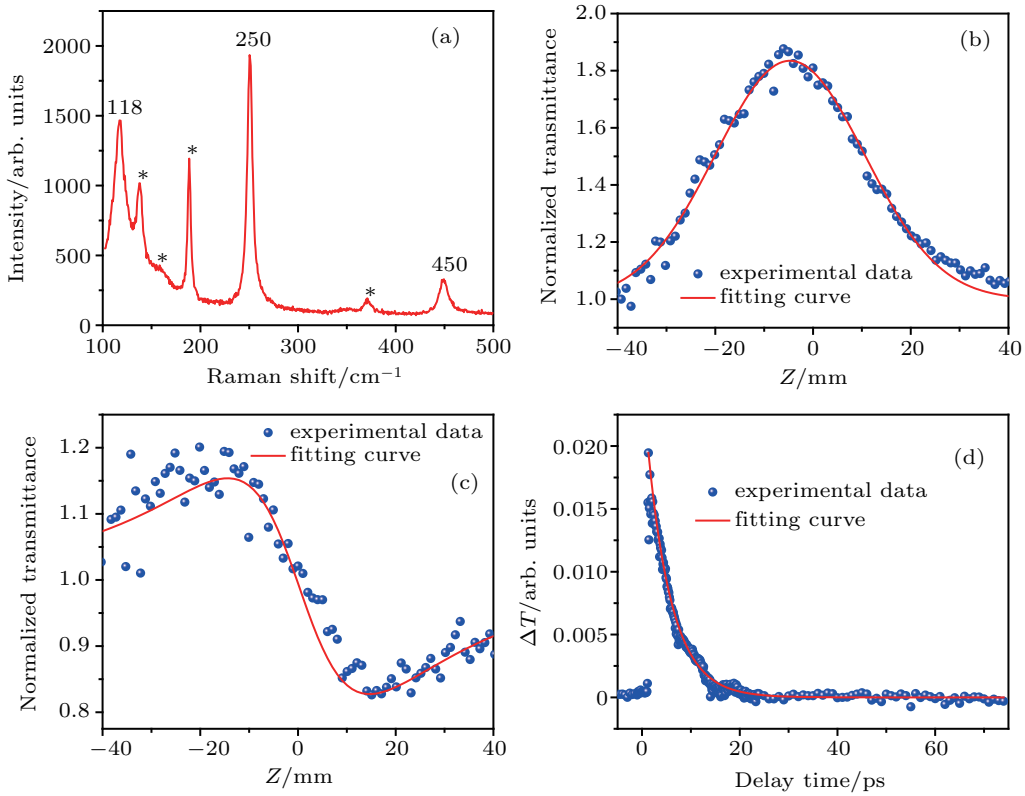


Fig. 1. (color online) (a) Raman spectrum of Sb_2Te_3 film. (b) The normalized open-aperture Z-scan trace. (c) The normalized CA/OA Z-scan trace. (d) Pump–probe measurement of the carrier lifetime of Sb_2Te_3.

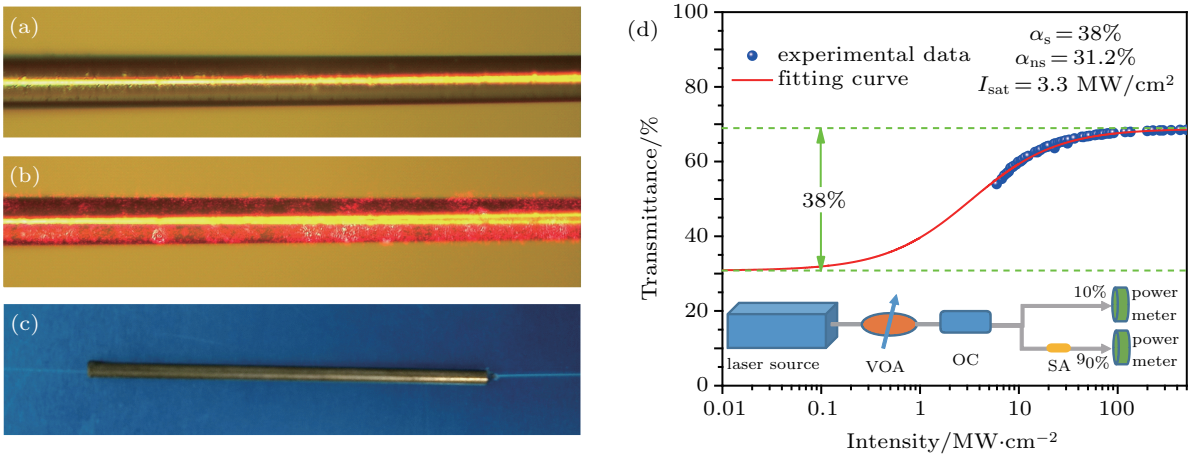


Fig. 2. (color online) Optical microscope images of the waist region of sample without (a) and with (b) the guiding 650-nm light. (c) A photograph of the prepared Sb_2Te_3 SA. (d) Saturable absorption property of SA. The inset was the schematics of the balanced twin-detector equipment.

Figures 2(a)–2(b) were the optical images of the microfiber coated with the Sb_2Te_3 material. The Sb_2Te_3-coated areas are clearly seen from the scattered light with a 650 nm visible light guided through the microfiber, indicating the strong Sb_2Te_3-light interaction through evanescent wave coupling effect. The Sb_2Te_3 SA will be slowly oxidized when it is exposed to the air, which is greatly detrimental for the performance of the SA. In order to solve this problem, as shown in Fig 2(c), we have insulated the tapered region coated with Sb_2Te_3 film from the air by packaging it into a small copper tube which is filled with nitrogen to ensure the high reliability and stability of the SA. The nonlinear optical absorption properties of microfiber-based Sb_2Te_3 SA is measured by a typical balanced twin-detector method with a configuration shown in the inset of Fig. 2(d). A homemade mode-locked fiber laser operating at central wavelength of 1864 nm with 1.3-ps pulse duration and fundamental frequency of 10.393 MHz was utilized as the test laser source. As shown in Fig. 2(d), the nonlinear saturable absorption curve is fitted by the two-level saturable absorber model

$$\alpha(I) = \frac{\alpha_s}{1 + I/I_{sat}} + \alpha_{ns}, \tag{5}$$

where $\alpha(I)$ is the absorption, I is the optical intensity, α_s is the modulation depth, α_{ns} is the nonsaturable loss, and I_{sat}

is the saturable intensity. In our experiment, the microfiber-based Sb_2Te_3 SA shows remarkable nonlinear properties with α_s, α_{ns}, and I_{sat} of 38%, 31.2%, and 3.3 MW/cm^2, respectively. Besides, the linear transmission of the fabricated absorber is also measured as $\sim$ 27.7% at 1900 nm by using the homemade amplified spontaneous emission (ASE) of Tm-doped gain fiber, and this result is basically in agreement with the fitting value obtained from the nonlinear saturable absorption measurement.

3. Schematic diagram of passively mode-locked fiber laser

We employed the microfiber-based Sb_2Te_3 SA in thulium-doped fiber (TDF) laser to further investigate its nonlinear optical properties. The experiment setup schematics is shown in Fig. 3. A 1550 nm/2000 nm wavelength-division multiplexer (WDM) is used to deliver the 1550-nm laser into the ring cavity. A piece of TDF (Nufern, SM-TSF-9/125) with the length of 3.2 m is used as the gain medium. An optical coupler (OC) with 50/50 splitting ratio is utilized to extract output pulses from the cavity. The total cavity length is about 14.2 m. A polarization controller (PC) is used to adjust the state of the polarization of the oscillating beam within the cavity, and a polarization insensitive optical isolator (PI-ISO) is used to prevent back reflection in the cavity and ensure unidirectional laser operation. Besides the TDF, the other fibers including the tail fibers of each element are SMF-28e fibers. All components are polarization-independent in the fiber laser systems, which can avoid the self-started mode-locking operation induced by nonlinear polarization evolution (NPE). It should be noted that the direction of the operating laser is opposite to that of the pump laser, which avoids the output of residual pump power.

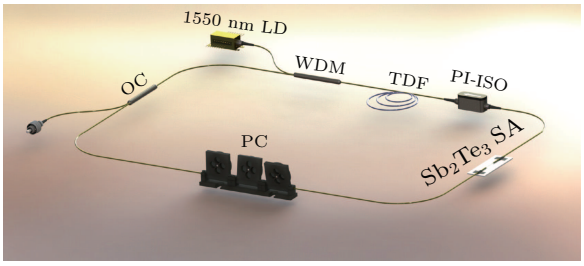


Fig. 3. (color online) Schematic diagram of passively mode-locked thulium doped fiber laser

The characteristics of the output light are monitored by an optical spectrum analyzer (Yokogawa AQ6375B) and an oscilloscope (ROHDE & SCHWARZ RTO2024) with a photo detector (EOT ET-5000 F), respectively. A radio frequency (RF) spectrum analyzer (ROHDE & SCHWARZ FSV13) is employed to record the RF spectrum of the mode-locking operation. In addition, the pulse duration is measured with a commercial autocorrelator (APE Pulsecheck).

4. Experimental results and discussion

Self-starting mode-locking operation is observed when the pump power reaches 400 mW. Compared with normal Er-doped fiber lasers,[43,44] our TDF laser exhibits a little higher lasing threshold due to the relatively large insertion loss caused by the small waist diameter of the microfiber which ensures sufficient evanescent field interaction to obtain stable mode-locking pulse operation. During operation, the pump power can be increased up to 1.5 W without losing the mode locking. The mode-locking performance is characterized at the maximum pump power of 1.5 W. Figure 4(a) shows the typical spectrum of mode-locking centered at 1930.07 nm with a 3-dB spectral bandwidth of 3.87 nm. The presence of Kelly sidebands on the spectrum confirmed that the mode-locked laser is operating in the soliton regime for typical all-anomalous dispersion lasers. The spectrum of output pulse is also measured from 1200 nm to 2000 nm and no signal is observed at 1550 nm, verifying that there is no output of residual pump power. Figure 5(b) shows the RF spectrum of the laser at a fundamental repetition rate of 14.51 MHz measured in a 0.6-MHz span with a 10-Hz resolution. The signal-to-noise ratio (SNR) is 84 dB. A wide 1-GHz span with a resolution of 1 kHz presented in the inset of Fig. 5(b) indicating the low fluctuations and the high stability of the mode locked pulse operation. The autocorrelation of the laser output pulse together with a sech^2 fitting is depicted in Fig. 5(c). The pulse duration after deconvolution is 1.24 ps. The time-bandwidth product (TBP) is calculated to be about 0.386, implying that the output pulses of our laser are slightly chirped. Additionally, the inset shows the autocorrelation trace with a large range of 50 ps, confirming the single-pulse operation without any pre- or post-pulses. The output average power is recorded in Fig. 5(d). The laser system produced a maximum average power of 130 mW at the pump power of 1.5 W, corresponding to the maximum pulse energy of 8.96 nJ. The slope efficiency is 11%. The large pulse energy is attributed to the microfiber-based Sb_2Te_3 SA with evanescent wave interaction which can avoid the transmittance of light through the SA material directly so as to prevent the dispersion caused by SA material efficiently and attractive for high power tolerance. The inset shows the oscilloscope trace of the pulse-train with the pulse interval of about 68.9 ns, well consistent with the cavity length.

Moreover, in order to examine the influence of the microfiber-based Sb_2Te_3 SA in thulium-doped mode-locked fiber laser system, we removed the Sb_2Te_3-SA and placed another uncoated microfiber with the same size. In this case, even if the PC is rotated and the pump power is adjusted gradually and carefully in a large range, the passively mode-locked pulse cannot be observed. The contrastive results demonstrate that the Sb_2Te_3-SA is responsible for the mode-locked operation.

The comparisons of mode-locked lasers operating at 2 μm based on different low-dimension materials are listed in Table 1. The output average power and the pulse energy are much larger than that mode locked by other low-dimensional materials, indicating that Sb_2Te_3 has significant advantages in obtaining high-power mode-locked fiber laser. These comparisons suggested that Sb_2Te_3 material may be served as an excellent SA at 2 μm that can successfully compete with other extensively studied low-dimensional materials such as carbon nanotube and graphene.

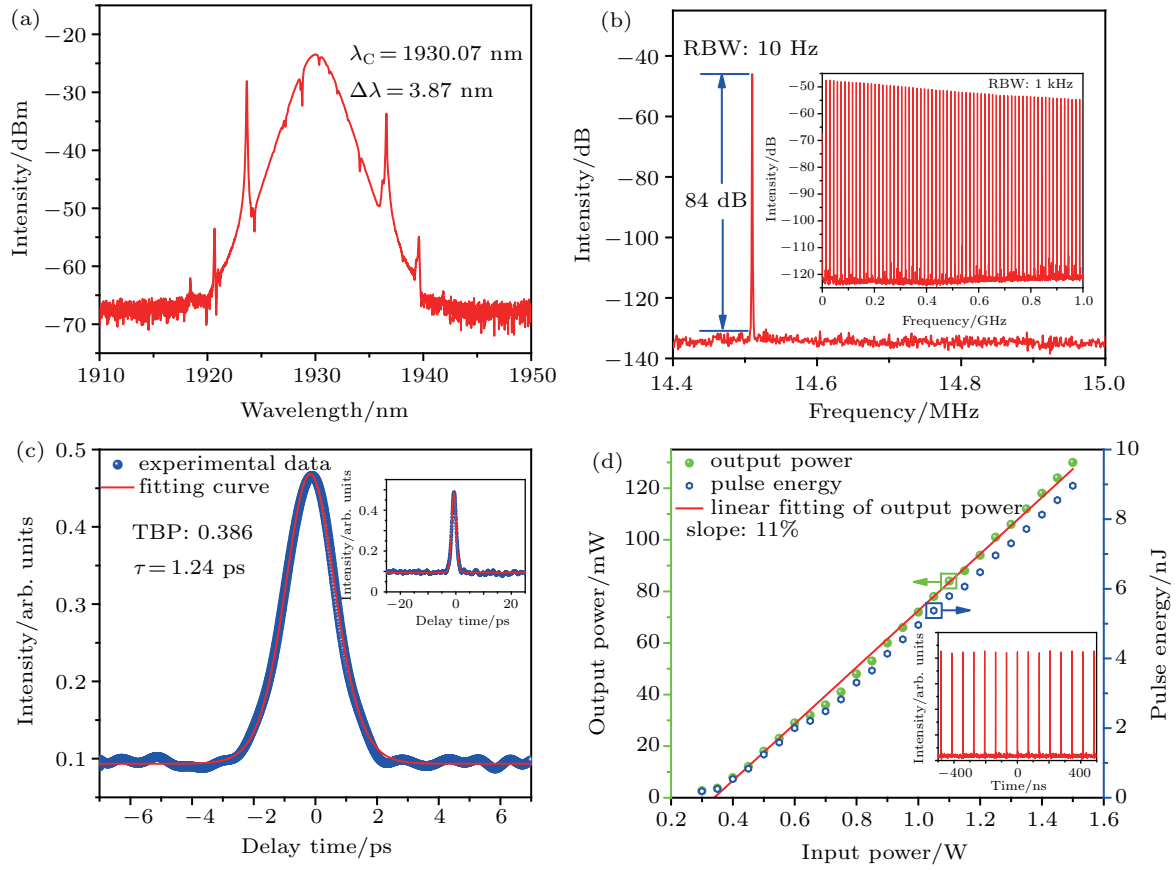


Fig. 4. (color online) (a) Optical spectrum with the bandwidth of 3.87 nm. (b) Radio frequency (RF) spectrum at fundamental frequency of 14.51 MHz with 10-Hz resolution. The inset was the RF spectrum of 1-GHz span. (c) Autocorrelation trace for output pulse with a pulse duration of 1.24 ps with $sech^2$ fit. The inset shows the autocorrelation trace with a large range of 50 ps. (d) Relationship between the pump power and output power. The inset is the oscilloscope trace of the pulse-train.

Table 1. Comparison of passively mode-locked fiber lasers around 2 μm.

SA	λ/nm	Δλ/nm	τ/ps	P_{avg}/mW	E/nJ	Reference
Carbon nanotube	1927	52.8	0.152	4.85	0.19	[4]
Graphene	1910	5.14	0.773	115	6	[21]
WSe_2	1863.96	3.19	1.16	32.5	2.86	[19]
Black Phosphorus	1910	5.8	0.739	1.5	0.04	[22]
Bi_2Te_3	1935	5.6	0.795	1	0.36	[32]
Sb_2Te_3	1930.07	3.87	1.24	130	8.96	this work

5. Conclusion

In conclusion, microfiber-based Sb_2Te_3 SA is prepared by MSD technique and its nonlinear optical properties are investigated. The microfiber-based Sb_2Te_3 SA is embedded into thulium-doped fiber laser with typically ring cavity structure. Stable soliton pulses emitting at 1930.07 nm are obtained with pulse duration of 1.24 ps, a 3-dB spectral bandwidth of 3.87 nm, an average power of 130 mW, and SNR of 84 dB. To our knowledge, this is the first demonstration of Sb_2Te_3-based SA in fiber lasers at 2-μm regime. Our results suggested that microfiber-based Sb_2Te_3 SA can be used as an excellent photonic device for ultrafast pulse generation in 2-μm regime, and MSD technique opens a promising way to produce high-performance SA with large modulation depth, low saturable intensity, and high power tolerance, which are beneficial for high power and ultrafast pulse generation with high stability.

References

[1] Woodward R and Kelleher E 2015 *Appl. Sci.* **5** 1440
[2] Wang P, Shi H, Tan F and Wang P 2017 *Opt. Express* **25** 16643
[3] Wu K, Wong J H, Shum P, Lim D R C S, Wong V K H, Lee K E K, Chen J and Obraztsova E D 2010 *Opt. Lett.* **35** 1085
[4] Wang J, Liang X, Hu G, Zheng Z, Lin S, Ouyang D, Wu X, Yan P, Ruan S and Sun Z 2016 *Sci. Rep.* **6** 28885
[5] Liu X, Han D, Sun Z, Zeng C, Lu H, Mao D, Cui Y and Wang F 2013 *Sci. Rep.* **3** 2718
[6] Ma J, Xie G, Lv P, Gao W, Yuan P, Qian L, Yu H, Zhang H, Wang J and Tang D 2012 *Opt. Lett.* **37** 2085
[7] Li J, Luo H, Wang L, Zhao C, Zhang H, Li H and Liu Y 2015 *Opt. Lett.* **40** 3659
[8] Luo Z Q, Li Y Y, Zhong M, Huang Y Z, Wan X J, Peng J and Weng J 2015 *Photon. Res.* **3** A79
[9] Luo Z C, Liu M, Guo Z N, Jiang X F, Luo A P, Zhao C J, Yu X F, Xu W C and Zhang H 2015 *Opt. Express* **23** 20030
[10] Zhang H, Lu S B, Zheng J, Du J, Wen S C, Tang D Y and Loh K P 2014 *Opt. Express* **22** 7249
[11] Zhang M, Richard C, Howe T, Woodward R I, Edmund J, Kelleher R, Torrisi F, Hu G, Popov S V and Taylor J R 2015 *Nano Res.* **8** 1522
[12] Mao D, Du B, Yang D, Zhang S, Wang Y, Zhang W, She X, Cheng H, Zeng H and Zhao J 2016 *Small* **12** 1489
[13] Sun Z P, Hasan T, Torrisi F, Popa D, Privitera G, Wang F Q, Bonaccorso F, Basko D M and Ferrari A C 2010 *Acs Nano* **4** 803
[14] Bao Q L, Zhang H, Ni Z H, Wang Y, Polavarapu L, Shen Z X, Xu Q H, Tang D Y and Loh K P 2011 *Nano Res.* **4** 297
[15] Yu H H, Zhang H, Wang Y C, Zhao C J, Wang B L, Wen S C, Zhang H J and Wang J Y 2013 *Laser Photon. Rev.* **7** L77
[16] Liu J, Wang Y G, Qu Z S, Zheng L H, Su L B and Xu J 2012 *Laser Phys. Lett.* **9** 15
[17] Yan P, Chen H, Liu A, Li K, Ruan S, Ding J, Qiu X and Guo T 2017 *IEEE J. Sel. Top. Quantum Electron.* **23** 33
[18] Yin J, Li J, Chen H, Wang J, Yan P, Liu M, Liu W, Lu W, Xu Z and Zhang W 2017 *Opt. Express* **25** 30020
[19] Wang J T, Lu W, Li J R, Chen H, Jiang Z K, Wang J Z, Zhang W F, Zhang M, Li I L, Xu Z H, Liu W J and Yan P G 2018 *IEEE J. Sel. Top. Quantum Electron.* **24** 1100706
[20] Wang J, Jiang Z, Chen H, Li J, Yin J, Wang J, He T, Yan P and Ruan S 2017 *Opt. Lett.* **42** 5010
[21] Jeong H, Choi S Y, Kim M H, Rotermund F, Cha Y H, Jeong D Y, Lee S B, Lee K and Yeom D I 2016 *Opt. Express* **24** 14152
[22] Sotor J, Sobon G, Kowalczyk M, Macherzynski W, Paletko P and Abramski K M 2015 *Opt. Lett.* **40** 3885
[23] Wang J, Chen H, Jiang Z, Yin J, Wang J, Zhang M, He T, Li J, Yan P and Ruan S 2018 *Opt. Lett.* **43** 1998
[24] Wang J, Jiang Z, Chen H, Li J, Yin J, Wang J, He T, Yan P and Ruan S 2018 *Photon. Res.* **6** 535
[25] Liu M, Zhao N, Liu H, Zheng X W, Luo A P, Luo Z C, Xu W C, Zhao C J, Zhang H and Wen S C 2014 *IEEE Photon. Technol. Lett.* **26** 983
[26] Wang Z T, Chen Y, Zhao C J, Zhang H and Wen S C 2012 *IEEE Photon. J.* **4** 869
[27] Song Y, Chen S, Zhang Q, Li L, Zhao L, Zhang H and Tang D 2016 *Opt. Express* **24** 25933
[28] Guo B, Yao Y, Yang Y F, Yuan Y J, Jin L, Yan B and Zhang J Y 2015 *Photon. Res.* **3** 94
[29] Guo B, Yao Y, Xiao J J, Wang R L and Zhang J Y 2016 *IEEE J. Sel. Top. Quantum Electron.* **22** 8
[30] Guo B, Lyu Q, Yao Y and Wang P 2016 *Opt. Mater. Express* **6** 2475
[31] Liu W, Pang L, Han H, Tian W, Chen H, Lei M, Yan P and Wei Z 2015 *Opt. Express* **23** 26023
[32] Jung M, Lee J, Koo J, Park J, Song Y W, Lee K, Lee S and Lee J H 2014 *Opt. Express* **22** 7865
[33] Wu K, Chen B, Zhang X, Zhang S, Guo C, Li C, Xiao P, Wang J, Zhou L, Zou W and Chen J 2018 *Opt. Commun.* **406** 214
[34] Xia H, Li H, Lan C, Li C, Zhang X, Zhang S and Liu Y 2014 *Opt. Express* **22** 17341
[35] Fan P, Zheng Z H, Liang G X, Cai X M and Zhang D P 2010 *Chin. Phys. Lett.* **27** 087201
[36] Sheik-Bahae M, Said A A, Wei T H, Hagan D J, Van Stryl and E W 1990 *IEEE J. Quantum Electron.* **26** 760
[37] Moreels I, Hens Z, Kockaert P, Loicq J and Van Thourhout D 2006 *Appl. Phys. Lett.* **89** 193106
[38] Liu Z, Wang Y, Zhang X, Xu Y, Chen Y and Tian J 2009 *Appl. Phys. Lett.* **94** 021902
[39] Jiang X, Liu S, Liang W, Luo S, He Z, Ge Y, Wang H, Cao R, Zhang F, Wen Q, Li J, Bao Q, Fan D and Zhang H 2018 *Laser Photon. Rev.* **12** 1700229
[40] Wang K, Wang J, Fan J, Lotya M, O'Neill A, Fox D, Feng Y, Zhang X, Jiang B, Zhao Q, Zhang H, Coleman J N, Zhang L and Blau W J 2013 *ACS Nano* **7** 9260
[41] Lu S B, Miao L L, Guo Z N, Qi X, Zhao C J, Zhang H, Wen S C, Tang D Y and Fan D Y 2015 *Opt. Express* **23** 11183
[42] Wei R, Zhang H, He X, Hu Z, Tian X, Xiao Q, Chen Z and Qiu J 2015 *Opt. Mater. Express* **5** 1807
[43] Chen H, Yin J, Yang J, Zhang X, Liu M, Jiang Z, Wang J, Sun Z, Guo T, Liu W and Yan P 2017 *Opt. Lett.* **42** 4279
[44] Yan P, Chen H, Yin J, Xu Z, Li J, Jiang Z, Zhang W, Wang J, Li I L and Sun Z 2017 *Nanoscale* **9** 1871